

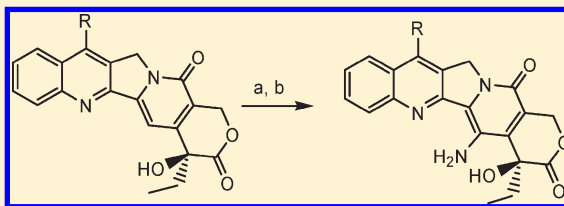
## 14-Aminocamptothecins: Their Synthesis, Preclinical Activity, and Potential Use for Cancer Treatment

Jian-Xin Duan,\* Xiaohong Cai, Fanying Meng, Jessica D. Sun, Qian Liu, Donald Jung, Hailong Jiao, Jackson Matteucci, Brian Jung, Deepthi Bhupathi, Dharmendra Ahluwalia, Heli Huang, Charles P. Hart, and Mark Matteucci

Threshold Pharmaceuticals, 1300 Seaport Blvd, Suite 500, Redwood City, California 94063, United States

## Supporting Information

**ABSTRACT:** 14-Aminocamptothecins were synthesized in good yields by treating camptothecin (**1a**) and 7-ethylcamptothecin (**1b**) with 90% fuming nitric acid either neat or in acetic anhydride and then followed by reduction of the resulting 14-nitrocamptothecins (**2**). 14-Aminocamptothecin (**3a**) and 7-ethyl-14-aminocamptothecin (**3b**) demonstrated excellent cytotoxic potency against human tumor cell lines in vitro, and they are not substrates for any of the major clinically relevant efflux pumps (MDR1, MRP1, and BCRP). **3a** and **3b** showed similar cytotoxicity against human and mouse bone marrow progenitor cells. This is in contrast to many camptothecin analogues, which are substrates for efflux pumps and are dramatically more toxic to human marrow cells relative to murine. **3a** and **3b** demonstrated significant brain penetration when dosed orally in mice. **3b** showed significantly better efficacy relative to topotecan when dosed orally in the three ectopic xenograft models, H460, HT29, and PC-3. On the basis of its favorable in vitro and in vivo profile, **3b** warrants future development.



## INTRODUCTION

Camptothecin was first isolated in 1966 by Wani and Wall.<sup>1</sup> Its potent cytotoxicity toward tumor cells and its discovery as an inhibitor of topoisomerase I, an essential enzyme for topological DNA modification during a number of critical cellular processes,<sup>2</sup> has stimulated extensive analogue investigations. Two camptothecin analogues, topotecan (**7**)<sup>3</sup> and irinotecan (**8**) (Figure 1),<sup>4</sup> are currently approved for the treatment of a variety of solid tumors, and many other analogues are currently in clinical trials. There continue to be active efforts to develop new camptothecin analogues that avoid the deficiencies of the currently approved drugs, such as being substrates for drug efflux pumps and having severe toxicity on human bone marrow progenitor cells.<sup>5</sup> The extensive historical SAR efforts have largely focused on the A, B, and E rings of camptothecin. Relatively few analogues of the D ring have been investigated; only one example at the 14 position with biological testing has been reported.<sup>6,7</sup> These data showed the 14-chloro derivative<sup>7</sup> was much less potent than the parent camptothecin, suggesting a lack of tolerance for substitution at that position. We developed a highly regioselective process for the synthesis of 14-nitro and 14-aminocamptothecin and their analogues and found that previously unknown 14-aminocamptothecins were surprisingly potent having approximately equal potency to the unsubstituted 14 position parent camptothecins.

## CHEMISTRY

Nitration of **1a** with a nitric and sulfuric acid mixture was first reported in 1986 by Wani and Wall<sup>8</sup> with a mixture of 9- and 12-substituted camptothecins being formed. The 14 position has previously been nitrated by using a large excess of nitronium

tetrafluoroborate in acetic anhydride, resulting in 20-O-acetyl-14-nitrocamptothecin being obtained at a 28% yield.<sup>9</sup> We found that nitration of **1b** went smoothly in acetic anhydride with 90% nitric acid at 0 °C, with **2b** being obtained as the only product (Scheme 1). This is in contrast to the completely different regiochemistry reported by Wani and Wall. The assignment of regiochemistry was based on the <sup>1</sup>H NMR spectra of the nitrocamptothecins. The <sup>1</sup>H NMR spectra of **1b** and **2b** are shown in Figure 2. The chemical shift of H-C<sub>14</sub> of **1b** appears at 7.33 ppm as a singlet in DMSO-*d*<sub>6</sub>, but this peak disappeared in the <sup>1</sup>H NMR spectrum of the corresponding nitro substituted product **2b**. The molecular weight of the product is consistent with **2b**. On the basis of this information, the product **2b** was identified as 7-ethyl-14-nitrocamptothecin.

The different regioselectivity observed with this procedure may be due to the fact that sulfuric acid (pK<sub>a</sub> = -3) is a very strong acid and is able to protonate the carbonyl group in the D ring in addition to protonation of the nitrogen in the B ring, thus deactivating the electrophilic substitution of the D ring (Scheme 1).

Reduction of **2a** and **2b** with H<sub>2</sub> in the presence of 10% Pd/C in methanol went smoothly at room temperature, and **3a** and **3b** were obtained in good yields (Scheme 2).

## RESULTS AND DISCUSSION

**Cytotoxicity Studies.** The compounds were screened for cytotoxicity using the H460 human non-small-cell lung cancer

Received: October 19, 2010

Published: February 22, 2011

(NSCLC) cell line, **1a**, 7-ethyl-10-hydroxycamptothecin (SN-38,<sup>4b</sup> the active metabolite of irinotecan **6**), and **7** were used as control compounds. Cells were treated with test compounds at various concentrations under air for 72 h, and cell viability and

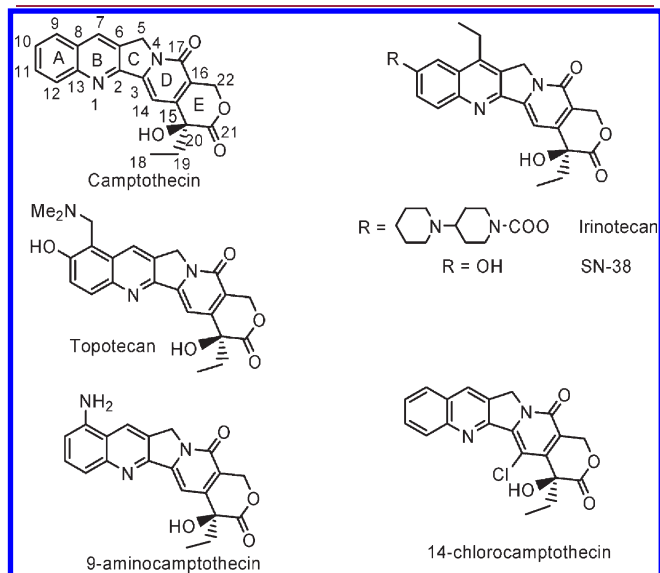


**Figure 1.** Structures of camptothecin, topotecan, irinotecan, SN-38, 9-aminocamptothecin, and 14-chlorocamptothecin.

proliferation were assessed by the resazurin-based AlamarBlue assay. The  $IC_{50}$  values for the tested compounds are shown in Table 1.

It has been reported that substitution on the 12 or 14 position will result in the loss of activity.<sup>6</sup> As expected, **2a** and **2b** were much less potent than **1a**. However, **3a** and **3b** were surprisingly potent, exhibiting potencies comparable to the approved camptothecin analogues, **6** and **7**, against the H460 cell line. After these intriguing results, these two compounds were tested against eight more human cancer cell lines with the *in vitro* cytotoxicity assay. The data listed in Table 1 show the potency of **3a** and **3b** are comparable to **6** and **7** across all the cell lines profiled.

It is well established that the camptothecin lactone, the biologically active form, is in equilibrium with the biologically inactive ring opened carboxylate.<sup>10,11</sup> However, this is not the case for 14-aminocamptothecins. As shown in Scheme 3, the lactones of **3a** and **3b** underwent ring-opening under basic conditions (NaOH/MeOH, rt, 4 h) to form their corresponding carboxylates **4a** and **4b**. Upon acidification, the carboxylates did not reform the lactones but instead formed the lactams, **5a** and **5b**, and no parent compounds **3a** and **3b** were detected. **5a** and **5b** were tested against the H460 cell line and were found to be several hundred-fold less active relative to **3a** and **3b** (Table 1).

The stability of **3a** and **3b** was determined in PBS with and without 40 mg/mL of human serum albumin (HSA) at 37 °C, pH 7.4, for up to 180 min. No hydrolysis of the lactones, **3a** and **3b**, was detected by LC/MS/MS. We conclude that **3a** and **3b**

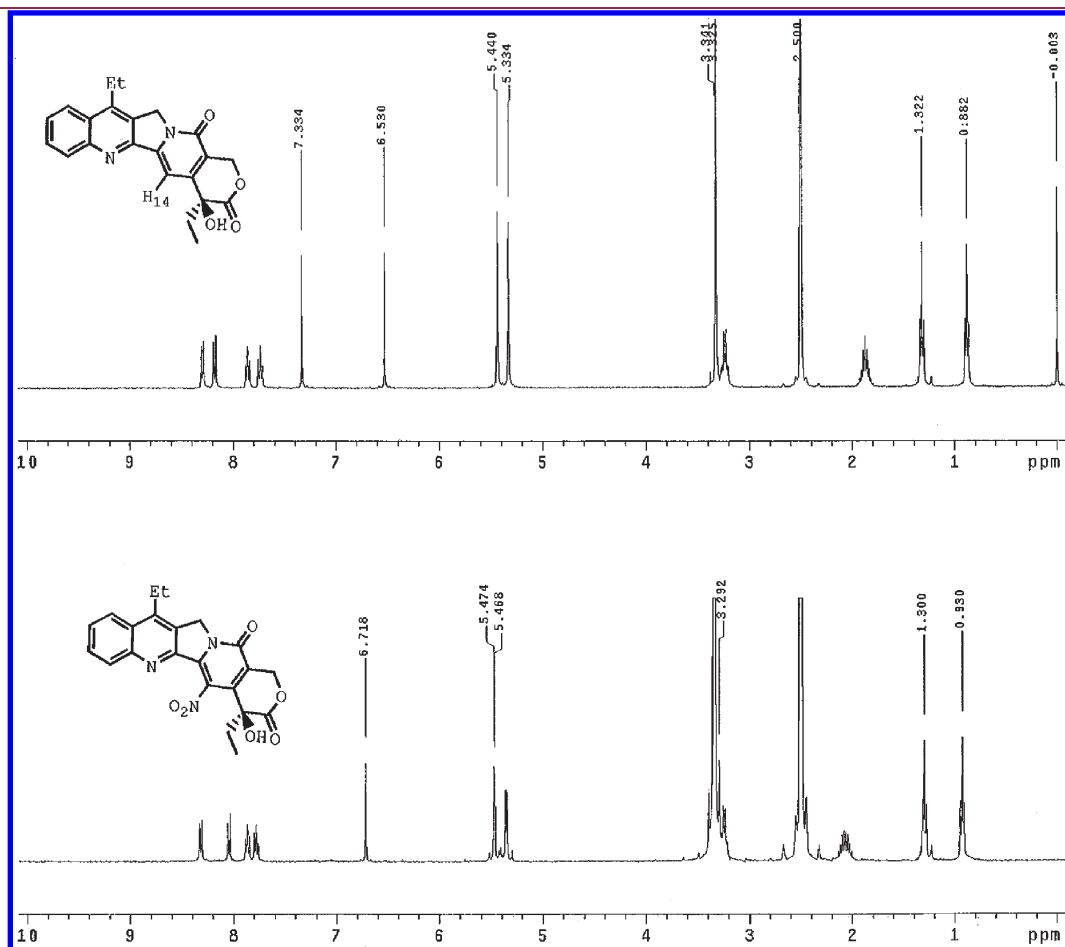
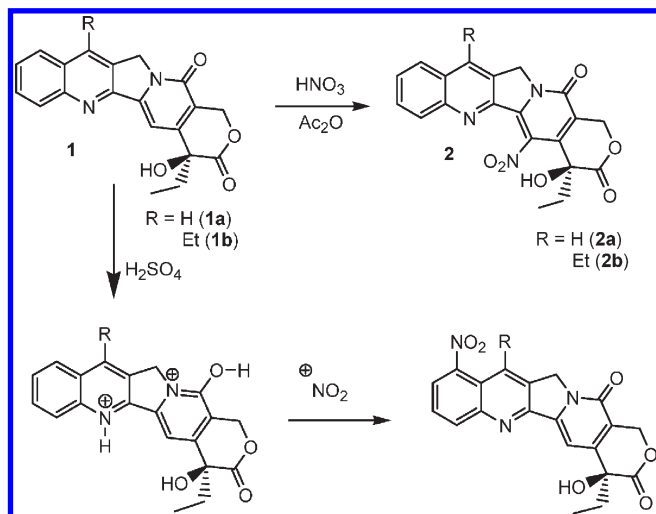
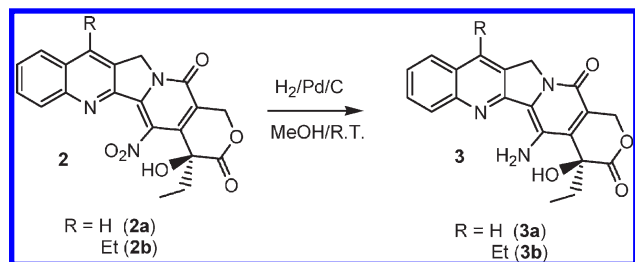


**Figure 2.** <sup>1</sup>H NMR spectra for **1b** and **2b**.

Scheme 1



Scheme 2



are very stable in the presence of physiological concentrations of HSA.

The cytotoxicity of **3a** and **3b** on the H460 cell line in the presence of 40 mg/mL of HSA showed that the activity of **3a** was reduced 5- to 10-fold, while the parent compound, **1a**, exhibited a reduction of more than 77-fold (Table 2). This shift of cytotoxicity may be due to the reversible binding of **3a** and **3b** to HSA. As expected, the potency of **6** and **7** were only slightly affected by the presence of HSA because the equilibrium of their lactone and carboxylate was not affected by HSA.<sup>12–14</sup>

**14-Aminocamptothecins Are Not Substrates for the Clinically Relevant Drug Resistant Pumps, MDR1, MRP1, and BCRP.** One of the main causes of treatment failure in cancer is the development of drug resistance. Increased efflux of drug by P-glycoprotein (P-gp, MDR1), multidrug resistance protein (MRP1), and breast cancer resistance protein (BCRP) limits the uptake of drug by tumor cells.<sup>15a</sup> Additionally, these pumps are responsible for decreasing oral bioavailability and brain penetration.<sup>15b</sup> **7** is a substrate of these three major drug resistant pumps (MDR1, MRP1, and BCRP), while **6** is a substrate of BCRP and MRP1.<sup>19</sup> To assess the liability of **3a** and **3b** to the drug resistant pumps, compounds were tested for cytotoxicity in efflux pump overexpressing cell lines versus the wild type cell lines from which the overexpressing lines were derived. The three pairs were MESSA and the MDR1 overexpressing cell line DX5,<sup>16</sup> H69 and the MRP1 overexpressing cell line H69AR,<sup>17</sup> and pcDNA and the BCRP overexpressing cell line BCRP (Table 3).<sup>18</sup> The results in Table 4 demonstrate that **3a** and

**3b** have similar activity against the three pairs of cell lines, while **1a** was a substrate of MRP1 and not a substrate of MDR1 and BCRP. Consistent with the published data, **7** is a substrate of all three efflux pumps and **6** is a substrate of the BCRP pump.<sup>19</sup>

**14-Aminocamptothecins Show Favorable Interspecies Bone Marrow Toxicity.** Many members of the camptothecin class have been shown to be highly efficacious in mice only to show excessive bone marrow toxicity in humans.<sup>20</sup> 9-Aminocamptothecin (**9**) displayed excellent *in vivo* antitumor activity in different mice xenografts and was investigated in a number of clinical trials.<sup>21</sup> However, it did not show promising antitumor activity in patients and the dose limiting toxicity was myelosuppression. The maximum tolerated dose in patients was much lower than was anticipated from mouse studies. A subsequent study found that bone marrow cells from humans are much more sensitive to **9** than those from mice.<sup>20</sup> The interspecies differences in the sensitivity of bone marrow cells to **3a** and **3b** was assessed by *in vitro* testing on human and mouse bone marrow-derived myeloid progenitor colony formation<sup>22,23</sup> (Table 4). On the basis of the  $\text{IC}_{50}$  values, **3a** and **3b** were much less toxic than the control compounds in both mouse and human bone marrow cells. The isomeric analogue of **3a**, compound **9**, was relatively less toxic to mouse bone marrow cells, having an  $\text{IC}_{50}$  of 90 nM against mouse bone marrow cells, which was about 8-fold more toxic relative to **3a** (710 nM) and **3b** (720 nM). When **9** was tested against human bone marrow cells, its toxicity was dramatically increased (over 50-fold), while **3a** and **3b** showed only a modest increase (4- and 7-fold shift for **3a** and **3b**, respectively). With the clinically approved agents, **7** and particularly **6**, the active metabolite of **8**, similar selective toxicity to human bone marrow progenitor cells was observed.

**Pharmacokinetic Studies: 3a and 3b Showed Significant Brain Penetration.** Compounds **7** and **8** have been approved to treat central nervous system (CNS) tumors and several other camptothecin analogues have been tested for treating glioblastoma in clinical trials.<sup>24</sup> The ability of **3a** and **3b** to reach the brain was tested in a mouse pharmacokinetic study. Following oral administration of **3a** and **3b** (50 mg/kg IP), peak plasma concentrations of 0.618 and 0.253  $\mu\text{g/mL}$ , respectively, were reached at 30 and 60 min post-dose and then declined biexponentially with half-lives of 250 min for each (Table 5). Peak concentrations of **3a** and **3b** in the brain were 0.6 and 0.3  $\mu\text{g/mL}$ , respectively, and declined in parallel to plasma concentrations with half-lives of 210 and 240 min. Time-averaged brain to plasma concentration ratios were 101% and 70% for **3a** and **3b**, respectively (Figure 3, Table 5).

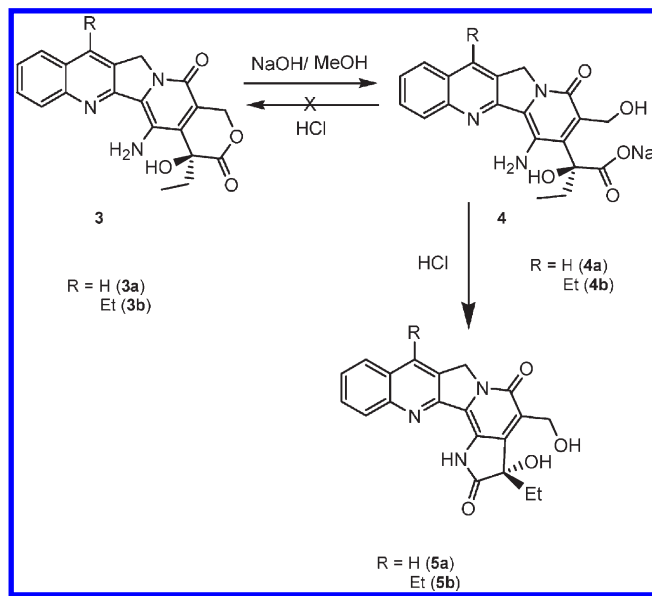
**Antitumor Activity of 3a and 3b in Ectopic Xenograft Models.** On the basis of the favorable *in vitro* data for **3a** and **3b**, their antitumor activities in the H460 (NSCLC) human tumor xenograft model were evaluated. H460 cells ( $1 \times 10^6$ ) were subcutaneously implanted in the flanks of pathogen-free homozygous female nude mice (nu/nu, Charles River Laboratories). When tumor size reached 100–150  $\text{mm}^3$ , animals were randomized to 10 mice per treatment group. All tested compounds were formulated in 5% DMSO, 5% Tween 80, and 1% CMC in water and were given orally by gavage. Doses and regimens are listed in Table 6. The doses of **3a** and **3b** were chosen on the basis of preliminary studies to define the MTD of each compound when administered daily for 5 days. On the basis of weight loss and behavioral signs, the MTDs of **3a** and **3b** were determined to be 30 and 40 mg/kg, respectively. Daily oral dosing of **7** was considered an optimal regimen and 2 mg/kg was used as an MTD.<sup>25</sup>

Table 1. Cytotoxicity Assay of 2, 3 and 5 with Human Tumor Cell Lines in Vitro<sup>a</sup>

	H460		PC-3		HT29		SK-MEL-2		A375		Malm-3M		DU 145		LNCaP		IGROV-1	
	IC <sub>50</sub> (nM)	95% CI	IC <sub>50</sub> (nM)	95% CI	IC <sub>50</sub> (nM)	95% CI	IC <sub>50</sub> (nM)	95% CI	IC <sub>50</sub> (nM)	95% CI	IC <sub>50</sub> (nM)	95% CI	IC <sub>50</sub> (nM)	95% CI	IC <sub>50</sub> (nM)	95% CI	IC <sub>50</sub> (nM)	95% CI
<b>1a</b>	14		12		260		140	90–250	13	8–16	1000	510–1800	30	14–36	9	1–11	160	55–220
<b>7</b>	45	23–50	45	17–40	>1000		100	46–190	4	2–6	200	62–330	4	2–6	9	4–13	30	13–74
<b>6</b>	54	30–68	4	2–5	220	46–540	170	120–190	22	14–26	780	410–810	50	20–71	110	70–180	120	55–190
<b>2a</b>	3000		43	18–32	230	96–320	130	61–170	7	4–12	1200	610–1600	18	10–30	120	51–190	20	4–29
<b>3a</b>	18	10–32	24	8–28	300	81–320												
<b>2b</b>	4600																	
<b>3b</b>	7	3–8																
<b>5a</b>	7700																	
<b>5b</b>	>10000																	

<sup>a</sup> H460: non-small-cell lung cancer cell line. HT29: colon cancer cell line. PC-3, DU 145, LNCaP: prostate cancer cell lines. SK-MEL-2, A375, Malm-3M: melanoma cell lines. IGROV-1: ovarian cancer cell line.

Scheme 3

Table 2. Effect of HSA on the Cytotoxic Potency of 1a and 3a and 3b<sup>a</sup>

	IC <sub>50</sub> (nM)				
	(- HSA)		( + HSA)		ratio
	IC <sub>50</sub> (nM)	95% CI	IC <sub>50</sub> (nM)	95% CI	
<b>1a</b>	13	8–18	>1000		>77
<b>7</b>	59	40–90	110	82–220	2
<b>6</b>	15	8–21	27	19–53	2
<b>3a</b>	23	15–36	120	93–320	5
<b>3b</b>	12	6–20	120	95–300	10

<sup>a</sup> H460 cell line in vitro.

In the H460 xenograft model, both **3a** and **3b** exhibited superior antitumor activity compared with **7** (Table 6 and Figure 4) when administered once daily for five consecutive days, followed by two days without treatment for two weeks (QD5 × 2). Treatment with **3a** and **3b** yielded 79% and 84% tumor growth inhibition (TGI) and 15 and 14 days tumor growth delay (TGD), respectively, with mean maximal body weight loss of about 4%. In the same model, **7** showed only a 46% TGI with a maximum body weight loss of 9%.

Both **3a** and **3b** showed similar antitumor activity in the H460 xenograft model. However, **3b** was much easier to formulate relative to **3a**, resulting in a homogeneous suspension for gavage using the 5% DMSO, 5% Tween 80, and 1% CMC in water formulation. Limited formulation experimentation with **3a** did not identify an improved formulation (data not shown), so subsequent efficacy models focused on **3b**.

**3b** was evaluated in the HT29 colon cancer and PC-3 prostate cancer xenograft models. In the HT29 xenograft model, **3b** exhibited a TGI of 101% and TGD of 30 days as compared to 70% TGI and a TGD of 16 days for **7**. In addition, 10 days after the last dose, 50% of the tumors (5/10) in the **3b** treated group had an objective response (OR) defined as tumors not growing for at least 10 days after the last dose. This is in contrast to 0%



(0/10) OR in the vehicle group and only 10% (1/10) in the 7 treated group.

In the PC-3 xenograft model, **3b** significantly inhibited tumor growth as compared to vehicle ( $p < 0.001$ ) and 7 ( $p < 0.05$ , one-way analysis of variance with Dunnett post-hoc test). TGI of **3b** and 7 were 107% and 79% and TGD was 46 and 21 days, respectively. Furthermore, the OR was 100% (10/10) for **3b** and 10% (1/10) for 7. **3b** showed mean maximal body weight loss of 7% with no animal exceeding 20% during treatment. Following

**Table 3. Drug Resistance Profiling of 3a and 3b on (a) MDR1, (b) MRP1, and (c) BCRP**

	(a) MDR1				
	MESSA		DXS		RR <sup>a</sup>
	IC <sub>50</sub> (nM)	95% CI	IC <sub>50</sub> (nM)	95% CI	
<b>1a</b>	57	40–66	52	30–64	1
7	4	1–10	33	13–57	8
6	10	6–12	22	13–29	2
<b>3a</b>	58	44–74	60	27–73	1
<b>3b</b>	4	2–6	12	6–22	3

	(b) MRP1				
	H69		H69AR		RR <sup>a</sup>
	IC <sub>50</sub> (nM)	95% CI	IC <sub>50</sub> (nM)	95% CI	
<b>1a</b>	1	1–4	>300		>250
7	6	1–8	>300		>47
6	22	7–36	250	69–380	11
<b>3a</b>	91	36–110	91	44–120	1
<b>3b</b>	110	54–230	240	67–290	2.2

	(c) BCRP				
	pcDNA		BCRP		RR <sup>a</sup>
	IC <sub>50</sub> (nM)	95% CI	IC <sub>50</sub> (nM)	95% CI	
<b>1a</b>	7	5–9	11	11–18	2
7	10	7–14	480		51
6	<1		220	17–400	>220
<b>3a</b>	7	6–11	14	9–31	2
<b>3b</b>	4	3–7	5	5–9	1

<sup>a</sup>RR: resistance ratio.

**Table 4. Human and Mouse CFU-GM: Interspecies in Vitro Hematologic Toxicity Difference<sup>a</sup>**

	CFU-GM (IC <sub>50</sub> )					CFU-GM (IC <sub>90</sub> )		
	mouse		human		ratio (Mo/Hu)	mouse		human
	IC <sub>50</sub> (nM)	95% CI	IC <sub>50</sub> (nM)	95% CI		IC <sub>90</sub> (nM)	IC <sub>90</sub> (nM)	ratio (Mo/Hu)
<b>9</b>	90	77–100	1	1–2	75	700	8	88
7	130	110–150	8	7–9	16	700	50	14
6	110	89–130	1	1–2	85	800	8	100
<b>3a</b>	710	450–970	10	50–210	6	4800	1100	4
<b>3b</b>	620	140–1100	110	72–130	6	4500	650	7

<sup>a</sup>IC<sub>50</sub> and IC<sub>90</sub> values derived from assays performed in triplicate.

treatment, body weight of the treated animals recovered rapidly. In all three models, the antitumor activity of **3b** was superior to 7 with daily oral dosing at maximum tolerated doses.

**Summary.** A highly regioselective method has been developed for synthesizing 14-aminocamptothecins. **3a** and **3b** demonstrated broad activity against tumor cells in vitro. **3b** and the clinically approved camptothecin analogue, 7, were directly compared by oral administration in three different human cancer xenograft models. **3b** demonstrated improved antitumor activity relative to 7 in all three models. Additionally **3b** possesses significant brain penetration, favorable efflux pump properties, and hematological toxicity profile. On the basis of these results, **3b** warrants advancement into clinical development.

## EXPERIMENTAL SECTION

<sup>1</sup>H and <sup>13</sup>C NMR spectra were recorded on a Varian 400 MHz spectrometer (400 and 75 MHz, respectively) using CDCl<sub>3</sub>, CD<sub>3</sub>OD, or DMSO-*d*<sub>6</sub> as solvents with TMS as an internal standard. HPLC was performed on an Agilent 1100 series. Mass spectra analysis was performed on an API 3000 mass spectrometer. Column chromatography was performed with silica gel (230–400 mesh). The purity of the final compounds, **2b**, **3a**, **3b**, **5a**, and **5b** were determined by LC/MS; due to the solubility limitation, the purity of **2a** could not be analyzed. The LC traces and the parameters for the LC/MS method are listed in the Supporting Information, and the purity of the final compounds **3a** and **3b** are more than 95% by HPLC. All chemicals were purchased from Sigma-Aldrich and Fisher Scientific.

**14-Nitrocamptothecin (2a).** At room temperature (rt), **1a** (2.0 g) was slowly added to a solution of nitric acid (90%, 20 mL) and the resulting mixture was then stirred overnight. After the reaction completion, the mixture was poured into ice-water (300 mL) and filtered under reduced pressure to yield a light-yellow solid. The solid was then washed with water (50 mL), methanol (50 mL), and ethyl ether (50 mL). 14-NO<sub>2</sub>-Camptothecin was obtained (1.0 g) as a light-yellow powder. <sup>1</sup>H NMR (DMSO-*d*<sub>6</sub>) δ 8.76 (s, 1H, H-7), 8.16 (d, *J* = 8.0 Hz, 1H, Ar), 8.05 (d, *J* = 8.4 Hz, 1H, Ar), 7.88 (t, *J* = 7.6 Hz, 1H, Ar),

**Table 5. Pharmacokinetics of 3a and 3b after a Single Oral Dose of 50 mg/kg IP to CD-1 Mice**

	3a		3b	
	plasma	brain	plasma	brain
<i>T</i> <sub>max</sub> (min)	30	30	60	60
<i>C</i> <sub>max</sub> (μg/mL)	0.6	0.6	0.3	0.3
AUC (μg·min/mL)	90	100	64	45
half-life (min)	250	210	250	240

7.76 (t,  $J = 7.4$  Hz, 1H, Ar), 6.74 (s, 1H, OH), 5.46 (s, 2H, H-17), 5.31 (s, 2H, H-15), 2.00–2.16 (m, 2H, CH<sub>2</sub> of 19-Et), 0.93 (t,  $J = 7.2$  Hz, 3H, CH<sub>3</sub> of 19-Et). <sup>13</sup>C NMR (DMSO-*d*<sub>6</sub>)  $\delta$  8.8, 31.4, 51.2, 65.7, 73.8, 120.9, 127.1, 128.6, 129.17, 129.23, 130.1, 130.8, 131.4, 132.4, 139.3, 141.7, 148.3, 150.4, 156.1, 171.3.

**7-Ethyl-14-nitrocampthothecin (2b).** At 0 °C, HNO<sub>3</sub> (1 mL) was slowly added to a suspension of **1b** (1.0 g) in Ac<sub>2</sub>O (30 mL) with vigorous stirring. After addition of HNO<sub>3</sub>, the reaction was stirred for one hour at 0 °C. Ac<sub>2</sub>O was then removed under reduced pressure, and the residue was dissolved in CH<sub>2</sub>Cl<sub>2</sub> and MeOH. The resulting clear solution was poured into water, and then CH<sub>2</sub>Cl<sub>2</sub> was removed under reduced pressure and filtered to yield a yellow solid. The solid was then washed with water and pure product was obtained as yellow powder (560 mg). The filtrate was concentrated, and the residue was purified by silica gel column chromatography (MeOH in CH<sub>2</sub>Cl<sub>2</sub> from 0 to 7%) to give 150 mg more of product, resulting in a total yield of 63.4%. <sup>1</sup>H NMR (DMSO-*d*<sub>6</sub>)  $\delta$  8.31 (d,  $J = 8.4$  Hz, 1H, Ar), 8.04 (d,  $J = 8.4$  Hz, 1H, Ar), 7.87 (t,  $J = 7.6$  Hz, 1H, Ar), 7.78 (t,  $J = 7.6$  Hz, 1H, Ar), 6.72 (s, 1H, OH), 5.47 (d,  $J = 2.4$  Hz, 2H, H-17), 5.35 (d,  $J = 6.0$  Hz, 2H, H-15), 3.24 (m, 2H, CH<sub>2</sub> of 7-Et), 2.00–2.16 (m, 2H, CH<sub>2</sub> of 19-Et), 1.30 (t,  $J = 7.4$  Hz, 3H, CH<sub>3</sub> of 7-Et), 0.93 (t,  $J = 7.4$  Hz, 3H, CH<sub>3</sub> of 19-Et). <sup>13</sup>C NMR (DMSO-*d*<sub>6</sub>)  $\delta$  8.8, 14.6, 22.9, 31.4, 50.4, 65.7, 73.8, 120.7, 124.6, 127.1, 127.2, 128.9, 129.0, 130.92, 130.95, 139.7, 141.7, 146.4, 148.8, 149.7, 156.0, 171.3. MS  $m/z$  422.3 (M + 1), 843.4 (2M + 1). C<sub>22</sub>H<sub>19</sub>N<sub>3</sub>O<sub>6</sub> mol wt 421.4.

**14-Aminocampthothecin (3a).** First, 200 mg of 10% Pd/C was added to a suspension of 560 mg of **2a** in MeOH (100 mL) at room temperature. Then the mixture was purged with nitrogen three times

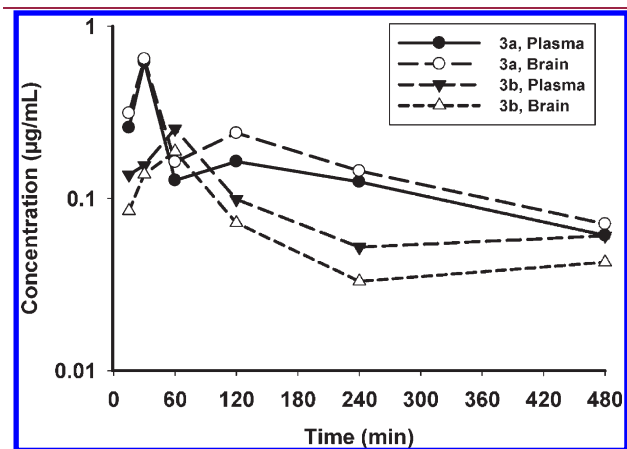


**Figure 3.** Pharmacokinetics of **3a** and **3b** after a single oral dose of 50 mg/kg IP to CD-1 mice.

and then connected to a balloon filled with hydrogen. After being stirred at room temperature for 3 h, Pd/C was removed by filtration and the filtrate was then concentrated under reduced pressure. The residue was purified by flash column purification (eluent: DCM:MeOH = 95:5 (V/V) to yield 460 mg of **3a**. <sup>1</sup>H NMR (DMSO-*d*<sub>6</sub>)  $\delta$  8.40 (s, 1H, 7-H), 8.00 (d,  $J = 8.0$  Hz, 1H, Ar), 7.95 (d,  $J = 8.0$  Hz, 1H, Ar), 7.74 (t,  $J = 7.6$  Hz, 1H, Ar), 7.57 (t,  $J = 7.4$  Hz, 1H, Ar), 7.00 (s, 1H, OH), 6.50 (s, 2H, NH<sub>2</sub>), 5.42 (d,  $J = 17.2$  Hz, 1H, H-17), 5.30 (d,  $J = 16.8$  Hz, 1H, H-17), 5.14 (s, 2H, H-15), 1.97–2.12 (m, 2H, CH<sub>2</sub> of 19-Et), 0.92 (t,  $J = 7.4$  Hz, 3H, CH<sub>3</sub> of 19-Et). <sup>13</sup>C NMR (DMSO-*d*<sub>6</sub>)  $\delta$  8.1, 30.2, 49.4, 65.8, 73.9, 121.8, 122.4, 126.2, 126.4, 128.1, 128.2, 128.7, 128.9, 129.9, 130.0, 136.6, 147.2, 152.8, 154.9, 171.9. MS  $m/z$  364.4 (M + 1), 727.8 (2M + 1). C<sub>20</sub>H<sub>17</sub>N<sub>3</sub>O<sub>4</sub> mol wt 363.4.

**7-Ethyl-14-aminocampthothecin (3b).** **2b** (1.0 g) was reduced with H<sub>2</sub> under same conditions as for **3a** to produce **3b** as a yellow powder at 73% yield. <sup>1</sup>H NMR (CDCl<sub>3</sub>)  $\delta$  8.11 (d,  $J = 8.4$  Hz, 1H, Ar), 8.04 (d,  $J = 8.0$  Hz, 1H, Ar), 7.73 (t,  $J = 7.6$  Hz, 1H, Ar), 7.58 (t,  $J = 7.6$  Hz, 1H, Ar), 6.48 (br, s, 2H, NH<sub>2</sub>), 5.78 (d,  $J = 16.8$  Hz, 1H, H-17), 5.26 (d,  $J = 16.8$  Hz, 1H, H-17), 5.22 (s, 2H, H-15), 4.30 (br, s, 1H, OH), 3.13 (q,  $J = 7.6$  Hz, 2H, CH<sub>2</sub> of 7-Et), 2.12–2.24 (m, 1H, CH<sub>2</sub> of 19-Et), 1.90–2.00 (m, 1H, CH<sub>2</sub> of 19-Et), 1.38 (t,  $J = 7.6$  Hz, 3H, CH<sub>3</sub> of 7-Et), 1.08 (t,  $J = 7.4$  Hz, 3H, CH<sub>3</sub> of 19-Et). <sup>13</sup>C NMR (DMSO-*d*<sub>6</sub>)  $\delta$  8.1, 13.7, 22.0, 30.2, 48.7, 65.8, 73.9, 121.6, 122.9, 123.6, 124.9, 126.3, 126.7, 128.6, 129.0, 129.4, 136.7, 143.6, 147.8, 152.8, 154.3, 172.0. MS  $m/z$  392.2 (M + 1), 783.7 (2M + 1). C<sub>22</sub>H<sub>21</sub>N<sub>3</sub>O<sub>4</sub> mol wt 391.4.

**5a.** At room temperature, NaOH (95 mg) was added to a solution of **3a** (100 mg, 0.265 mmol) in MeOH and the reaction mixture was stirred at room temperature for one hour. TLC showed that the starting material disappeared completely. The resulting solution was then acidified with concentrated HCl to a pH of 2. The cyclization of the carboxylate **4a** to **5a** completed within 10 min (monitored by TLC). After removing the solvent under reduced pressure, the residue was dissolved in CH<sub>2</sub>Cl<sub>2</sub> and washed with brine. The organic layer was then dried over MgSO<sub>4</sub>, filtered, and concentrated under reduced pressure. After silica gel column chromatography purification (eluent: acetone in toluene from 20 to 100%), a 32% yield was obtained. <sup>1</sup>H NMR (DMSO-*d*<sub>6</sub>)  $\delta$  10.67 (s, 1H), 8.54 (s, 1H), 8.17 (d,  $J = 8.4$  Hz, 1H), 8.05 (d,  $J = 8.4$  Hz, 1H), 7.83 (t,  $J = 7.6$  Hz, 1H), 7.65 (t,  $J = 7.6$  Hz, 1H), 6.41 (s, 1H), 5.26 (s, 2H), 5.08 (t,  $J = 5.2$  Hz, 1H), 4.66 (m, 2H), 2.14–2.01 (m, 2H), 0.67 (t,  $J = 7.4$  Hz, 3H). <sup>13</sup>C NMR (DMSO-*d*<sub>6</sub>)  $\delta$  7.9, 30.9, 50.4, 54.2, 119.7, 122.6, 126.9, 128.8, 128.9, 129.2, 130.7, 144.6, 144.8, 148.1, 152.8, 158.9, 177.5. MS  $m/z$  364.2 (M + 1), 726.4 (2M + 1). C<sub>20</sub>H<sub>17</sub>N<sub>3</sub>O<sub>4</sub> mol wt 363.4.

**5b.** **5b** was synthesized as described for **5a** in 38% yield. <sup>1</sup>H NMR (DMSO-*d*<sub>6</sub>)  $\delta$  10.63 (s, 1H), 8.19 (t,  $J = 6.8$  Hz, 2H), 7.81 (t,  $J = 7.6$  Hz, 1H), 7.66 (t,  $J = 7.6$  Hz, 1H), 6.41 (s, 1H), 5.28 (s, 2H), 5.08 (t,  $J = 5.2$  Hz, 1H), 4.66 (m, 2H), 3.16 (q,  $J = 7.6$  Hz, 1H), 2.12–2.034 (m, 2H),

**Table 6.** In Vivo Antitumor Activity in Ectopic Xenograft Models<sup>a</sup>

xenograft model	compd	dosage (mg/kg)	dosing regimen	TGI (%)	TGD (days)	max BW loss (%)
H460 NSCLC	7	2	QD5 × 2	46	5	9
	3a	30	QD5 × 2	79	15	4
	3b	40	QD5 × 2	84	14	4
HT29 colon cancer	7	2	QD5 × 4	70	16	0
	3b	40	QD5 × 4	101	30	3
PC-3 prostate cancer	7	2	QD5 × 2	79	21	1
	3b	40	QD5 × 2	107	45	8

<sup>a</sup> 1 cycle: QD, 5 days on/2 days off, oral route of administration (po). TGI: tumor growth inhibition =  $(1 - \Delta T/\Delta C) \times 100$ , where  $\Delta T/\Delta C$  presented the ratio of the change in mean tumor volume of the treated group and of the control group; TGD: tumor growth delay was calculated as the extra days for the treated tumor to reach 500 mm<sup>3</sup> as compared to the control group.

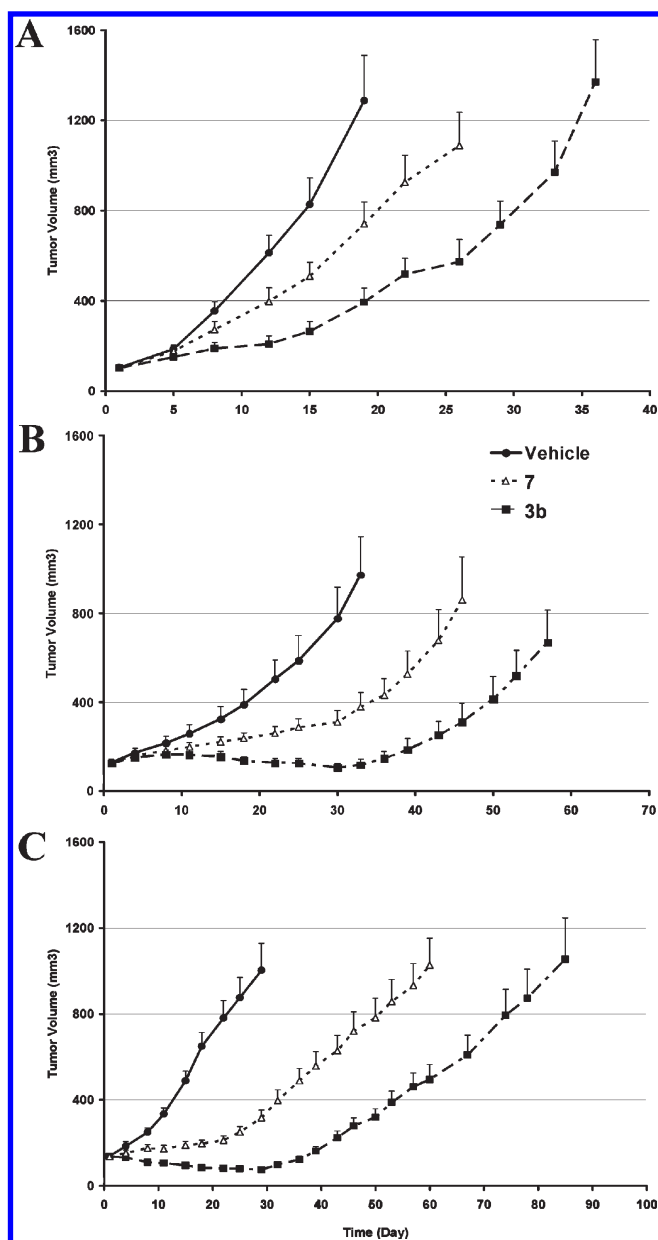


**Figure 4.** Growth of sc implanted human xenografts in nude mice treated with vehicle, 7, or 3b in (A) H460 NSCLC, (B) HT29 colon cancer, and (C) PC-3 prostate cancer xenograft models. Doses and regimens are listed in Table 6. Mean  $\pm$  SE for group of 10 mice.

1.30 ( $t, J = 7.6$  Hz, 3H), 0.66 ( $t, J = 7.4$  Hz, 3H).  $^{13}\text{C}$  NMR (DMSO- $d_6$ )  $\delta$  7.9, 13.9, 22.1, 30.9, 38.5, 49.7, 54.1, 76.6, 119.7, 123.2, 123.8, 125.6, 126.9, 127.2, 128.8, 129.5, 129.7, 144.6, 144.8, 148.6, 152.2, 158.9, 177.5. MS  $m/z$  392.2 ( $M + 1$ ), 783.7 ( $2M + 1$ ).  $\text{C}_{22}\text{H}_{21}\text{N}_3\text{O}_4$  mol wt 391.4.

**In Vitro Human Tumor Cell Line Cytotoxicity Assay.** In vitro proliferation assays were conducted as described by Meng et al.<sup>26</sup> In brief, exponentially growing cells were seeded at a density of  $4 \times 10^3$  cells per well in a 96-well plate and incubated at 37 °C in 5%  $\text{CO}_2$ , 95% air, and 100% relative humidity for 24 h prior to addition of test compounds. Compounds were solubilized in 100% DMSO at 200 times the desired final test concentration. At the time of drug addition, compounds were further diluted to 4 times the desired final concentration with complete medium. Aliquots of 50  $\mu\text{L}$  of compound at specified concentrations were added to microtiter wells already containing 150  $\mu\text{L}$  of medium,

resulting in the final drug concentration reported. After drug addition, the plates were incubated for an additional 72 h at 37 °C, 5%  $\text{CO}_2$ , 95% air, and 100% relative humidity. At the end of this incubation, the viable cells were quantified using the AlamarBlue assay. The drug concentration resulting in growth inhibition of 50% ( $\text{IC}_{50}$ ) was calculated using Prism software (Irvine, CA).

For cells treated with human serum albumin (HSA), 40 mg/mL of HSA was added to cells and cocultured with compounds for 72 h.

**Ex Vivo Hematological Toxicity CFU-GM Assay.** Human bone marrow cells derived from normal bone marrow were thawed on the day of experiments. Normal mouse bone marrow was extracted from both femurs on the day of experiments. The culture was set up in triplicate at  $2 \times 10^4$  cells per culture for both human and mouse progenitor cells. Clonogenic progenitors granulocyte–monocyte (CFU-GM) lineages were assessed in a semisolid methylcellulose-based medium (R&D Systems) containing recombinant rhSCF (50 ng/mL), rhIL-3 (10 ng/mL), and rhGM-CSF (10 ng/mL). Clonogenic progenitors of the mouse erythroid (BFU-E) and myeloid (CFU-GM) lineages were assessed in a methylcellulose based system (R&D Systems) containing rmSCF (50 ng/mL), rmIL-3 (10 ng/mL), and rhIL-6 (10 ng/mL). Following 10–12 days in culture, the mouse progenitor derived colonies were assessed and scored. Following 16–18 days in culture, the human progenitor derived colonies were assessed and scored.

**Brain and Plasma Concentrations of 3a and 3b in CD-1 Mice.** CD-1 mice weighing approximately 25 g were dosed intraperitoneally with 50 mg/kg of 3a or 3b in a vehicle consisting of 5% DMSO and 5% Tween 80 in water for injection. Blood from individual mice (three per time point) for pharmacokinetic analysis were collected by cardiac puncture into EDTA tubes at different times up to 480 min, mixed, and centrifuged for 5 min at 13000g to obtain plasma. Immediately following collection of the blood, individual whole brains from each animal were excised, washed with distilled water, patted dry, flash frozen in dry ice/acetone, and then weighed. Plasma and brain samples were stored at  $-70$  °C until analysis. Plasma samples were treated with five volumes of ice cold acetonitrile containing 1  $\mu\text{g}/\text{mL}$  of propranolol followed by vortex mixing for 30 s to precipitate proteins. Following centrifugation for 20 min at 3000g, 5  $\mu\text{L}$  of the supernatant was injected onto a HPLC/MS/MS triple quadrupole mass spectrometer (Sciex API3200 QTRAP). A BetaBasic 4, 5  $\mu\text{m}$  HPLC column (2.1 mm  $\times$  50 mm) from Thermo Fisher Scientific (Waltham, MA) was used to separate the drugs and the internal standard, propranolol. To whole brains, four volumes of water were added and homogenized in a Precellys-24 (Bertin Technologies, Saint Quentin en Yvelines Cedex, France) for two cycles of 15 s each. The resulting brain homogenate was then treated with four volumes of ice cold acetonitrile containing 1  $\mu\text{g}/\text{mL}$  of propranolol, centrifuged for 20 min at 3000g, and 5  $\mu\text{L}$  of the resultant supernatant was injected onto the HPLC/MS/MS system described above.

**Effect of HSA on the Lactone–Lactam Ratios.** The kinetics of conversion and the equilibrium concentrations of the lactone and lactam forms of the camptothecins 3a, 3b, 5a, and 5b were measured at pH 7.4 in PBS with and without 40 mg/mL HSA. Stock solutions (10 mM) of the drugs were diluted to 10  $\mu\text{M}$  and incubated for up to 180 min. Triplicate samples of 50  $\mu\text{L}$  each were immediately treated with four volumes of ice-cold acetonitrile followed by vortex mixing for 30 s to precipitate proteins and extract the total lactone and lactam forms of the drugs. Following centrifugation for 20 min at 3000g, 5  $\mu\text{L}$  of the supernatant was injected onto the HPLC/MS/MS system as described above.

**In Vivo Human Tumor Xenograft Models and Antitumor Activity.** Specific pathogen-free homozygous female (male for prostate cancer models) nude mice (nu/nu, Charles River Laboratories) were used. Mice were given food and water ad libitum and housed in microisolator cages. Four to six week old animals were identified by microchips (Locus Technology, Manchester, MD, USA) at the time of



the experiments. All animal studies were approved by the Institutional Animal Care and Use Committee at Threshold Pharmaceuticals, Inc.

All cell lines were from the American Type Culture Collection (ATCC, Rockville, MD, USA). Cells were cultured in the suggested medium with 10% fetal bovine serum and maintained in a 5% CO<sub>2</sub> humidified environment at 37 °C.

For ectopic models, cells were mixed with Matrigel (50% in HT29 and PC-3, 30% in H460) and 0.2 mL per mouse were subcutaneously implanted to the flank area of the animals (Table 1). When tumor size reached 100–150 mm<sup>3</sup>, mice were randomized into experimental or vehicle groups with 10 mice/group and treatment was started (day 1). **3a**, **3b**, and **7** were formulated in 5% DMSO, 5% Tween 80, and 1% CMC in water. All compounds were given orally by gavage, QD × 5/wk (5 days on, 2 days off) as one cycle, for a total of 2 or 4 cycles. MTD (maximal tolerated dose) was determined in the earlier studies as following: **3a** at 30 mg/kg, **3b** at 40 mg/kg, and **7** at 2 mg/kg. Tumor growth and body weight were measured twice a week. Tumor volume was calculated as (length × width<sup>2</sup>)/2. Drug efficacy was assessed as tumor growth inhibition (TGI) and tumor growth delay (TGD). TGI was defined as  $(1 - \Delta T/\Delta C) \times 100$ , where  $\Delta T/\Delta C$  presented the ratio of the change in mean tumor volume of the treated group and of the control group. TGD was calculated as the extra days for the treated tumor to reach 500 mm<sup>3</sup> as compared to the control group. Animals were culled when individual tumor size reached over 2000 mm<sup>3</sup> or mean tumor volume exceeded 1000 mm<sup>3</sup> in the group. Data are expressed as the mean ± SEM. One-way analysis of variance with Dunnett post-hoc test (GraphPad Prism 4) or two-tailed student's *t*-test were used for analysis. A *P* level <0.05 was considered statistically significant.

## ■ ASSOCIATED CONTENT

Supporting Information. <sup>1</sup>H NMR, <sup>13</sup>C NMR spectra and LC/MS of **2a**, **2b**, **3a**, **3b**, **5a**, and **5b** and the purities of **2b**, **3a**, **3b**, **5a**, and **5b** from reverse phase HPLC analysis. This material is available free of charge via the Internet at <http://pubs.acs.org>.

## ■ AUTHOR INFORMATION

### Corresponding Author

\*Phone: 650-474-8231. Fax: 650-474-0408. E-mail: [jduan@thresholdpharm.com](mailto:jduan@thresholdpharm.com).

## ■ ACKNOWLEDGMENT

We thank Dr. Emer Clarke of ReachBio, Seattle, WA, for performing the CFU-GM assays and Zhijun Ye for help with the NMR spectra of the compounds and Marci Robison for help on the preparation of the manuscript.

## ■ ABBREVIATIONS USED

BCRP, breast cancer resistance protein; BW, body weight; CPT, camptothecin; GM-CFU, granulocyte macrophage colony-forming unit; HSA, Human serum albumin; IC<sub>50</sub>, the half maximal inhibitory concentration; MDR1, multidrug resistance 1; MRP1, multidrug resistance protein 1; MTD, maximum tolerated dose; NSCLC, non small cell lung cancer; OR, objective response; PBS, phosphate buffered saline; SAR, structure activity relationship; TGD, tumor growth delay; TGI, tumor growth inhibition

## ■ REFERENCES

(1) Wall, M. E.; Wani, M. C.; Cook, C. E.; Palmer, K. H.; McPhail, A. T.; Sim, G. A. Plant antitumor agents. I. The isolation and structure of

camptothecin, a novel alkaloidal leukemia and tumor inhibitor from *Camptotheca acuminata*. *J. Am. Chem. Soc.* **1966**, *88*, 3888–3890.

(2) Wang, J. C. DNA topoisomerases. *Annu. Rev. Biochem.* **1996**, *65*, 635–692.

(3) Kingsbury, W. D.; Boehm, J. C.; Jakas, D. R.; Holden, K. G.; Hecht, S. M.; Gallagher, G.; Caranfa, M. J.; McCabe, F. L.; Faucette, L. F.; Johnson, R. K.; Hertzberg, R. P. Synthesis of water-soluble (aminoalkyl)camptothecin analogues: inhibition of topoisomerase I and antitumor activity. *J. Med. Chem.* **1991**, *34*, 98–107.

(4) (a) Negoro, S.; Fukuoka, M.; Masuda, M.; Kusunoki, Y.; Matsui, K.; Takifuji, N.; Kudoh, S.; Niitani, H.; Taguchi, T. Phase I study of weekly intravenous infusions of CPT-11, a new derivative of camptothecin, in the treatment of advanced non-small-cell lung cancer. *J. Natl. Cancer Inst.* **1991**, *83*, 1164–1168. (b) Kawato, Y.; Aonuma, M.; Hirota, Y.; Kuga, H.; Sato, K. Intracellular roles of SN-38, a metabolite of the camptothecin derivative CPT-11, in the antitumor effect of CPT-11. *Cancer Res.* **1991**, *51*, 4187–4191.

(5) Basili, S.; Moro, S. Novel camptothecin derivatives as topoisomerase I inhibitors. *Expert Opin. Ther. Pat.* **2009**, *19*, 555–574.

(6) Zunino, F.; Dallavalle, S.; Laccabue, D.; Beretta, G.; Merlini, L.; Pratesi, G. Current status and perspectives in the development of camptothecins. *Curr. Pharm. Des.* **2002**, *8*, 2505–2520.

(7) Sawada, S.; Matsuoka, S.; Nokata, K.; Nagata, H.; Furuta, T.; Yokokura, T.; Miyasaka, T. Synthesis and antitumor activity of 20(S)-camptothecin derivatives: A-ring modified and 7,10-disubstituted camptothecins. *Chem. Pharm. Bull.* **1991**, *12*, 3183–3188.

(8) Wani, M. C.; Nicholas, A. W.; Wall, M. E. Plant antitumor agents. 23. Synthesis and antileukemic activity of camptothecin analogues. *J. Med. Chem.* **1986**, *29*, 2358–2363.

(9) Cao, Z. Preparation of 14-nitrocamptothecin derivatives by reactions of camptothecin with nitronium tetrafluoroborate in acidic solvents. *J. Chem. Soc., Perkin Trans. 1* **1996**, *21*, 2629–2632.

(10) Hertzberg, R. P.; Caranfa, M. J.; Holden, K. G.; Jakas, D. R.; Gallagher, G.; Mattern, M. R.; Mong, S.-M.; Bartus, J. O.; Johnson, R. K.; Kingsbury, W. D. Modification of the hydroxylactone ring of camptothecin: inhibition of mammalian topoisomerase I and biological activity. *J. Med. Chem.* **1989**, *32*, 715–720.

(11) Giovanella, B. C.; Hinz, H. R.; Kozielski, A. J.; Stehlin, J. S., Jr.; Silber, R.; Potmesil, M. Complete growth inhibition of human cancer xenografts in nude mice by treatment with 20-(S)-camptothecin. *Cancer Res.* **1991**, *51*, 3052–3055.

(12) Burke, T. G.; Munshi, C. B.; Mi, Z.; Jiang, Y. The important role of albumin in determining the relative human blood stabilities of the camptothecin anticancer drugs. *J. Pharm. Sci.* **1995**, *84*, 518–519.

(13) Loos, W. J.; Verweij, J.; Gelderblom, H. J.; DeJonge, M. J.; Brouwer, E.; Dallaire, B. K.; Sparreboom, A. Role of erythrocytes and serum proteins in the kinetic profile of total 9-amino-20(S)-camptothecin in humans. *Anticancer Drugs* **1999**, *10*, 705–710.

(14) Mi, Z.; Malak, H.; Burke, T. G. Reduced albumin binding promotes the stability and activity of topotecan in human blood. *Biochemistry* **1995**, *34*, 13722–13728.

(15) (a) Ling, V. Multidrug resistance: molecular mechanisms and clinical relevance. *Cancer Chemother. Pharmacol.* **1997**, *40* (Suppl), S3–S8. (b) Ayrton, A.; Morgan, P. Role of transport proteins in drug absorption, distribution and excretion. *Xenobiotica* **2001**, *31*, 469–497.

(16) Harker, W. G.; Sikic, B. I. Multidrug (pleiotropic) resistance in doxorubicin-selected variants of the human sarcoma cell line MES-SA. *Cancer Res.* **1985**, *45*, 4091–4096.

(17) Hipfner, D. R.; Gauldie, S. D.; Deeley, R. G.; Cole, S. C., P. Detection of the M(r) 190,000 multidrug resistance protein, MRP, with monoclonal antibodies. *Cancer Res.* **1994**, *54*, 5788–5792.

(18) Robey, R. W.; Honjo, Y.; Morisaki, K. Mutations at aminoacid 482 in the ABCG2 gene aVect substrate and antagonist specificity. *Br. J. Cancer* **2003**, *89*, 1971–1978.

(19) Kruijtzter, C. M. F.; Beijnen, J. H.; Schellens, J. H. M. Improvement of oral drug treatment by temporary inhibition of drug transporters and/or cytochrome P450 in the gastrointestinal tract and liver: an overview. *The Oncologist* **2002**, *7*, 516–530.



(20) Erickson-Miller, C. L.; May, R. D.; Tomaszewski, J.; Osborn, B.; Murphy, M. J.; Page, J. G.; Parchment, R. E. Differential toxicity of camptothecin, topotecan and 9-aminocamptothecin to human, canine, and murine myeloid progenitors (CFU-GM) in vitro. *Cancer Chemother. Pharmacol.* **1997**, *39*, 467–472.

(21) (a) Kirichenko, A. V.; Rich, T. A.; Newman, R. A.; Travis, E. L. Potentiation of murine MCA-4 carcinoma radio response by 9-amino-20-(S)-camptothecin. *Cancer Res.* **1997**, *57*, 1929–1933. (b) Lamond, J. P.; Mehta, M. P.; Boothman, D. A. The potential of topoisomerase I inhibitors in the treatment of CNS malignancies: report of a synergistic effect between topotecan and radiation. *J. Neurol.—Oncol.* **1996**, *30*, 1–6.

(22) Masubuchi, N.; May, R. D.; Atsumi, R. A predictive model of human myelotoxicity using five camptothecin derivatives and the in vitro colony-forming unit granulocyte/macrophage assay. *Clin. Cancer Res.* **2004**, *10*, 6722–6731.

(23) Kurtzberg, L. S.; Battle, T.; Rouleau, C.; Bagley, R. G.; Agata, N.; Yao, M.; Schmid, S.; Roth, S.; Crawford, J.; Krumbholz, R.; Ewesuedo, R.; Yu, X. J.; Wang, F.; Lavoie, E. J.; Teicher, B. A. Bone marrow and tumor cell colony-forming units and human tumor xenograft efficacy of noncamptothecin and camptothecin topoisomerase I inhibitors. *Mol Cancer Ther.* **2008**, *7*, 3212–3222.

(24) (a) Avgeropoulos, G. N.; Batchelor, T. T. New treatment strategies for malignant gliomas. *Oncologist* **1999**, *4*, 209–224. (b) Feun, L.; Savaraj, N. Topoisomerase I inhibitors for the treatment of brain tumors. *Expert Rev. Anticancer Ther.* **2008**, *8* (5), 707–716.

(25) Li, T.-K.; Houghton, J. P.; Desai, D. S.; Daroui, P.; Liu, A. A.; Hars, S. E.; Ruchelman, L. A.; LaVoie, J. E.; Liu, F. L. Characterization of ARC-111 as a novel topoisomerase I-targeting anticancer drug. *Cancer Res.* **2003**, *63*, 8400–8407.

(26) Meng, F.; Ngnyen, X.-T.; Cai, X.; Duan, J.; Matteucci, M.; Hart, C. P. ARC-111 inhibits hypoxia-mediated hypoxia-inducible factor-1 $\alpha$  accumulation. *Anti-Cancer Drugs* **2007**, *18* (4), 435–445.